Table 1 Sequences of primer pairs used for reverse-transcription polymerase chain reaction (*CTGF* connective tissue growth factor, *GAPDH* glyceraldehyde-3-phosphate dehydrogenase)

Gene	Sequence	Annealing temperature (°C)	Products (bp)	Accession number or reference
Collagen type I	Forward 5′-GATCCTGCTGACGTGGCCAT Reverse 5′-ACTCGTGCAGCCGTCGTAGA	55	212	AY350905
Collagen type III	Forward 5′-TCCCCAGCAAAAGATTTCAC Reverse 5′-AGCACCATTGAGACATTTGAA	45	237	AJ289758
Bone sialoprotein	Forward 5′-ACTGAAGCCCAAGGAACCAC Reverse 5′-TCCAACGTGGTCTTCTGGAC	48	480	L10363
Runx2/cbfa1	Forward 5′-GACCCTGGAAGGAAACACAA Reverse 5′-CGCTGGTCCATGCTTAGAGT	56	303	Iohara et al. 2004
Osteocalcin	Forward 5′-TCAACCCCGACGACGAG Reverse 5′-GACCGTCGACRAAACCCTGA	60	204	AY150038
Osteopontin	Forward 5′-GCAATGAGCATTCCAATGTG Reverse 5′-GACCGTCGACTAAACCCTGA	56	383	X16575
Periostin	Forward 5′-CTGCACATGCAAGGATGACT Reverse 5′-ACATGGAGTTTCCCAGGCTA	54	589	AY880669
Biglycan	Forward 5′-GATGGCCTGAAGCTCAA Reverse 5′-GGTTGTTGAAGAGGCTG	60	406	AF159382
CTGF	Forward 5′-GCTCTTCTTCATGACCTCACCGT Reverse 5′-GCGGCTTACCGACTGGAAGACAC	60	411	U70060
GAPDH	Forward 5′-TCGACCACAGGGTAGGTTTC Reverse 5′-CCCCAGCATCAAAGGTAGAA	45	497	AF017079

Measurement of cell proliferation

DFC-I were plated at a density of 5×10^3 cells/ml into 6-well Col-I-d and standard tissue-grade P-d (BD Biosciences, Mountain View, Calif.). The DFC-I in each well were counted by using a WST-8 kit (Cell-counting Kit-8; Dojindo Laboratories, Kumamoto, Japan). The counting technique employed a tetrazolium salt that produces a highly water-soluble formazan dye. After a 1-h incubation with reagent according to the manufacturer's instructions, the relative cell number was determined by measuring the absorbance of light at a wavelength of 450 nm at days 1, 7, and 14 (Model 650 Microplate Reader; Biorad Laboratories, Hercules, Calif.).

Assay for ALPase activity

DFC-I were plated at density of 5×10^3 cells/ml into 6-well Col-I-d and P-d (BD Biosciences). For quantitative analysis of ALPase activity, *p*-nitrophenol production was measured at 37°C for 6 min in Milli-Q water by using a Fast *p*-

Table 2 Sequence of primer pairs for real-time polymerase chain reaction (*GAPDH* glyceraldehyde-3-phosphate dehydrogenase)

Gene	Sequence	Annealing temperature (°C)	Products (bp)	Accession number
Collagen type I	Forward 5′-TCAAAGTCTTCTGCAACATGGAG Reverse 5′-GGCACGCTGGGCTGAG	61	79	AY350905
Collagen type III	Forward 5′-TTGGCCCTGTTTGCTTTTTATAA Reverse 5′-CAAAAGGAACACATATGGAGTGTGA	61	82	AJ289758
Bone sialoprotein	Forward 5′-CCGAGGCCGAGAATATCACTC Reverse 5′-TTCCCGGCGTTACGTCC	61	66	L10363
Osteocalcin	Forward 5′-CTGGCTGATCACATCGGCT Reverse 5′-GCGAGGTCTAGGCTATGCCAT	61	64	AY150038
Osteopontin	Forward 5′-GCTGTCCCCACGGGAGA Reverse 5′-TTTTGACCTCAGTCCATAGACCAC	61	66	X166575
Periostin	Forward 5′-GGTCACAGACGTGGATTGGAT Reverse 5′-CCAGTTGGAGCTGTAGCCACT	61	71	AY880669
Biglycan	Forward 5′-AACGGGAGCCTGAGTTTTCTG Reverse 5′-CACCCTGGACAGCTTGTTGTT	61	69	AF159382
GAPDH	Forward 5′-GGGTCATCATCTCTGCCCCT Reverse 5′-CTCATGGTTCACGCCCACT	61	68	AF017079

nitrophenyl phosphate tablet set (Sigma) as a substrate. The relative amount of *p*-nitrophenol was estimated from the light absorbance at a wavelength of 405 nm at days 1, 7, and 14 (Bio-Rad Laboratories).

In vivo differentiation assay

The differentiation potential of individual DFC-I on transplantation into immunodeficient mice was assessed as described previously (Handa et al. 2002). Briefly, 1.5×10^6 DFC-I were incubated in a mixture of 40 mg β-tricalcium phosphate powder (TCP; Osferion G1, no. BH064005, Olympus Biomaterials, Tokyo, Japan) and fibrin clot (mixture of mouse fibrinogen and thrombin; both from Sigma) and were then inoculated subcutaneously into 5-week-old female CB-17 scid/scid (scid; severe combined immunodeficiency) mice (Nihoncrea, Tokyo, Japan). Mice were sacrificed after 1, 2, 4, and 8 weeks. The implants removed at 1, 2, and 4 weeks after transplantation were cut in half for histochemical analysis, calcification analysis, and mRNA expression analysis of periodontium matrix components. The implants removed at 8 weeks after transplantation were only used for histological analysis.

At 4 and 8 weeks after transplantation, the implants were fixed, decalcified with 10% EDTA-2Na, and then processed for histological examination by using standard procedures. Sections were stained with hematoxylin-eosin for histological observation and prepared for immunohistochemistry.

Immunohistochemical analysis was performed by using the Vectastain ABC kit (Vector Laboratories), as previously described (Hsu et al. 1981) with modification (Chen et al. 1991a). The antibody used was an affinity-purified rabbit anti-pig BSP polyclonal antibody (gift from Dr. J. Sodek, University of Toronto, Canada) (1:2,000 dilution). To determine the potential for hard tissue formation in the DFC-I, we selected 15 sections at random from at least five specimens.

The Von Kossa staining procedure was also performed to analyze the extent of calcification in hard tissue, as described previously (Piattelli et al. 1994).

Results

Porcine third molar at early crown-formation stage

The 6-month porcine third molar appeared at the crown-formation stage (Fig. 1a), with the formation of hard tissues being well advanced. The DF was clearly distinguished from the dental enamel organ and enamel at high magnifi-

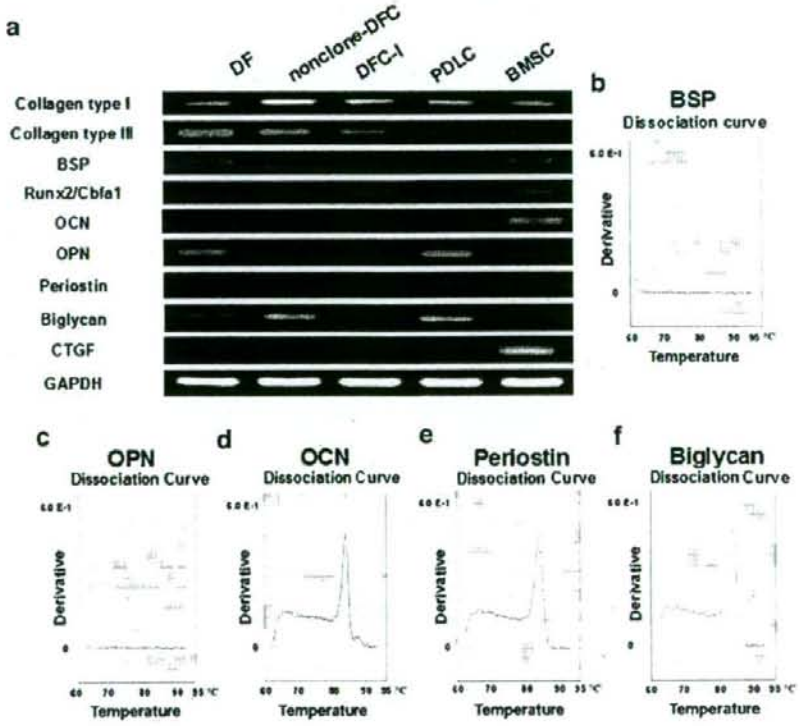

Fig. 3 **a** Semiquantitative RT-PCR analysis of osteoblast-lineage/periodontal ligament-related genes in DF, nonclone-DFC, DFC-I, PDLC, and BMSC. In DFC-I, there was no detectable expression of mature cementoblast/osteoblast markers such as bone sialoprotein (*BSP*), osteopontin (*OPN*), osteocalcin (*OCN*), connective tissue growth factor (*CTGF*), and biglycan, and no periostin. The expression of OPN, biglycan, and BMP-4 was higher in PDLC than in BMSC, but Runx2/Cbfa1, CTGF, and ALPase showed lower expression in PDLC than in BMSC. **b–f** Melting profile of the amplicon of BSP, OPN, OCN, periostin, and biglycan in DFC-I by real-time RT-PCR. Results were obtained by using the Sequence Detection Systems of dissociation curve software. OCN, periostin, and biglycan expressions were detected in DFC-I, but BSP and OPN were not detected

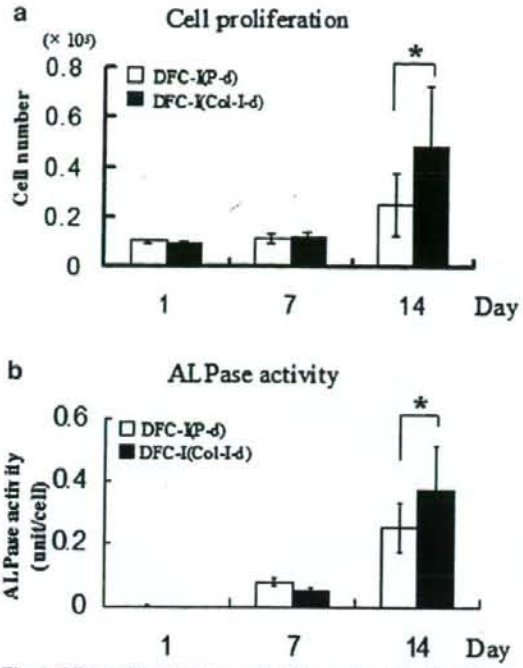

Fig. 4 Effects of Col-I matrix on DFC-I on cell proliferation (**a**) and ALPase activity (**b**). The cells were seeded at a density of 5.0×10^3 cells in standard 6-well plates (*P-d*) or in 6-well plates coated by Col-I (*Col-I-d*). No significant differences were apparent at 1 and 7 days. At 14 days, cell proliferation and ALPase activity of DFC-I cultured on Col-I-d were significantly higher than those on P-d. *Statistically significant at $P<0.05$ (paired *t*-test)

cation by the increased collagen fibrils occupying the extracellular spaces between the follicular fibroblasts (Fig. 1b). ECM in the DF was positive for the Col-I mesenchymal marker by immunohistochemistry (Fig. 1c).

Immunofluorescent staining of DFC

Immunofluorescent staining was then carried out to determine the lineage of the isolated cells by using antibodies specific for vimentin (Fig. 1d) and Col-I (Fig. 1e) as mesenchymal markers, and an anti-cytokeratin14 antibody as an epithelial marker (Fig. 1f). All isolated cells were positive for Col-I and vimentin and negative for cytokeratin14 (nuclei showed blue DAPI staining). These results demonstrated that all isolated cells were derived from mesenchyme with no contamination from dental epithelial cells.

Purification of DFC

One DFC-I colony was expanded and analyzed over a number of weeks in culture, producing a cumulative expansion in the single cell clones for over 30 passages prior to the onset of cellular senescence. Overall, six clones were expanded; the other clones exhibited only moderate growth potential that did not persist beyond 20 passages. The DFC-I comprised polygonal cells (Fig. 2a,b), whereas both the PDLC (Fig. 2c,d) and BMSC (Fig. 2e,f) had a mixed morphology including spindle-shaped and polygonal-shaped cells.

Gene expression pattern of DFC-I

We surveyed gene expression patterns in the DF, nonclone-DFC, DFC-I, PDLC, and BMSC by sq-PCR analysis (Fig. 3a). A series of genes are known to be involved in the morphogenesis of periodontium and bone (Table 1). The expression patterns of three DF-related genes in the DF, nonclone-DFC, and DFC-I were markedly different. mRNA expression for BSP and osteopontin (OPN) was only detected in the DF. Biglycan was expressed only in the DF and nonclone-DFC. From these results, the expression pattern of DFC-I resembled the more immature stage. Differences were also found when we compared the gene expression profiles of DFC-I, PDLC, and BMSC. BSP, OCN, and connective tissue growth factor (CTGF) expression was detected only in BMSC, whereas OPN, periostin, and biglycan were expressed only in the PDLC and BMSC. Runx2/Cbfa1 mRNA was expressed in all cell types. The expression levels of GAPDH were consistent across samples. BSP, OCN, OPN, periostin, and biglycan were not detected in DFC-1 by sq-PCR, prompting further investigation by rt-PCR for these genes (Table 2). Surprisingly, cementoblast/osteoblast markers such as BSP and OPN were not detected in DFC-I, but periostin, biglycan,

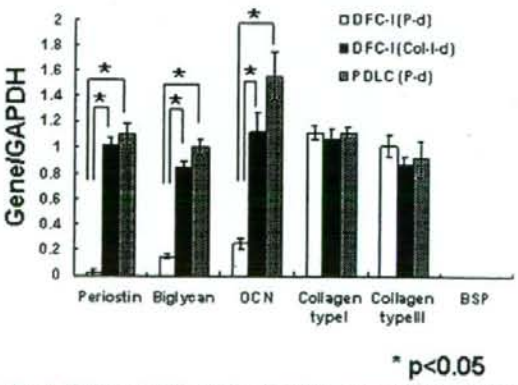

Fig. 5 Effects of Col-I matrix on mRNA expressions in DFC-I cultured on P-d and Col-d and in PDLC on P-d as measured by using real-time RT-PCR. DFC-I cultured on Col-I-d showed upregulated gene expression of periostin, biglycan, and OCN, whereas BSP were not expressed in any of the three cell classes. The results were consistent within three independent experiments. *Statistically significant at $P<0.05$ (paired *t*-test)

and OCN were expressed, albeit at a lower level in DFC-I than in PDLC and BMSC (Fig. 3b–f). These data suggested that DFC-I represented more immature cells compared with PDLC and BMSC.

Effect of Col-I matrix on cell proliferation and ALPase activity

After 1 and 7 days in culture, the cell proliferation of DFC-I cultured on Col-I-d was similar to that on P-d. After 14 days, DFC-I cultured on Col-I-d showed a significantly higher rate of cell proliferation compared with clones cultured on P-d (Fig. 4a). ALPase activity is a recognized mineralization marker in tissue (Alliot-Licht et al. 2005; Pavasant et al. 2003). The DFC-I cultured for 1, 7, and 14 days exhibited different and increasing levels of ALPase activity (Fig. 4b). At days 1 and 7 of culture, the ALPase activity change was the same regardless of culturing conditions, but at 14 days, DFC-I cultured on Col-I-d showed higher activity than those cultured on P-d (Fig. 4b). This

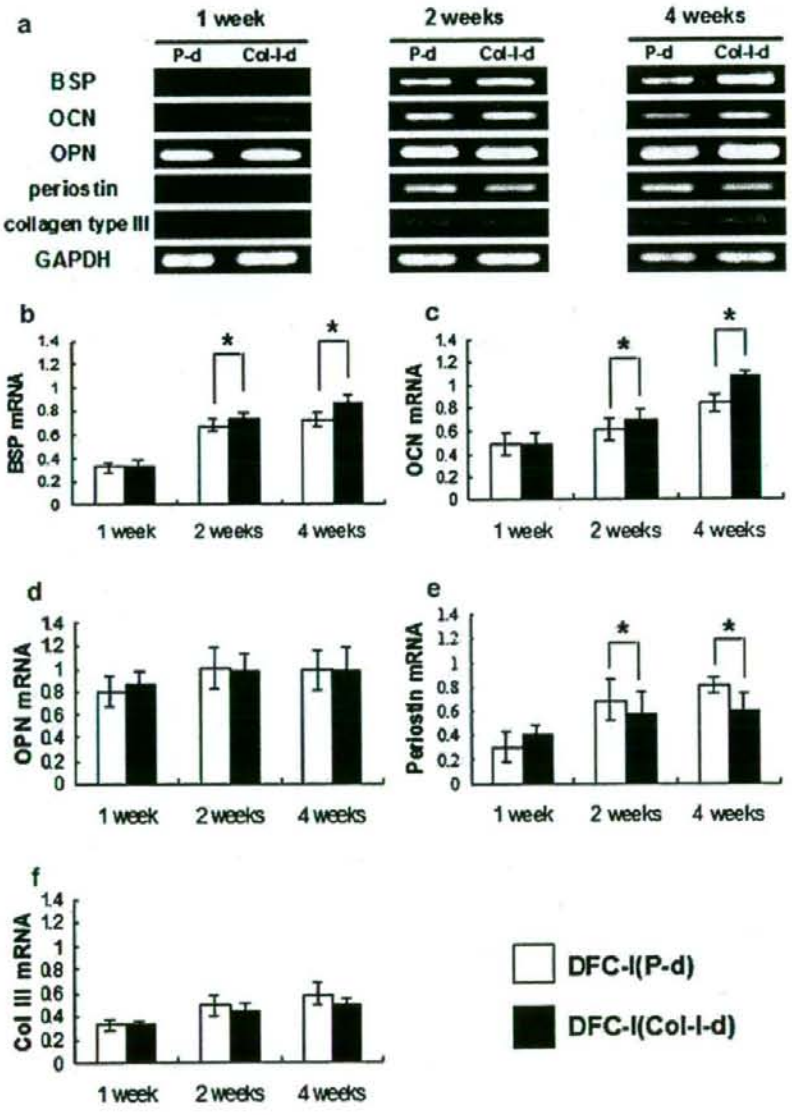

Fig. 6 Effects of Col-I matrix on gene expressions in DFC-I in vivo. **a** At 1 week, the BSP, periostin, and collagen type III genes were not expressed in either implant type but were clearly expressed at 2 and 4 weeks after transplantation. OCN and OPN genes were expressed strongly in both implant types at all time points. **b–f** Quantification of expression of BSP, OCN, OPN, periostin, and collagen type III genes by using Scion picture-imaging software. BSP and OCN genes were more highly expressed in the implants cultured on Col-I-d than in those on P-d at 2 and 4 weeks. In contrast, periostin expression was higher in implants on P-d at 2 and 4 weeks than in those cultured on Col-I-d. No significant difference in the expressions of OPN and collagen type III was seen for both implant types at all time points. *Statistically significant at $P<0.05$ (paired t-test)

result suggested that adhesion to Col-I promoted differentiation of the DFC-I.

Effect of Col-I on gene expressions in clone-DFC-I

We next investigated, by rt-PCR, the effect of Col-I culturing on gene expression in the DFC-I cells (Fig. 5). Putative markers of PDLC and cementoblasts/osteoblasts, such as periostin, biglycan, and OCN, were amplified more readily from DFC-I cultured on Col-I compared with DFC-I cultured on P-d. Periostin, biglycan, and OCN expression levels in DFC-I cultured on Col-I-d were approximately 100-fold, 6-fold, and 5-fold higher, respectively, than in DFC-I cultured on P-d. The expression levels of upregulated genes resembled levels of the same genes in PDLC, whereas the expression levels of Col-I and collagen type III showed no change, even in DFC-I cultured on Col-I. BSP was not expressed in DFC-I cultured on P-d or Col-I-d, or

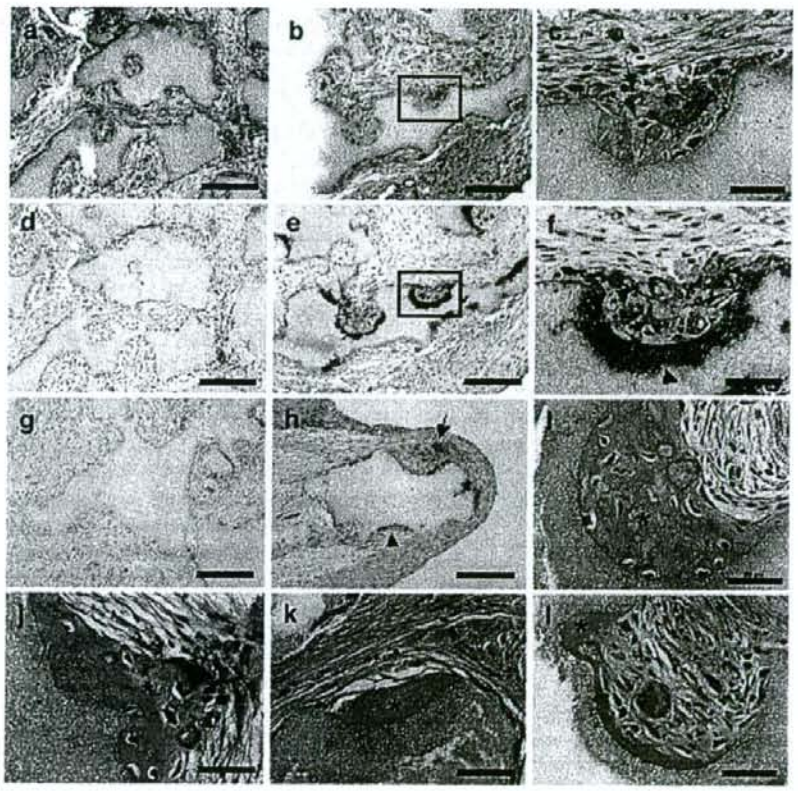

Fig. 7 **a–h** Morphology of representative implants of DFC-I cultured on P-d (**a**, **d**, **g**) or Col-I-d (**b**, **c**, **e**, **f**, **h**), at 4 weeks after transplantation. **a** No hard tissue formation was seen in the implants from P-d. Connective tissues were formed between the TCP particles. **b** A small amount of the hard tissue was produced in the implants from DFC-I cultured on Col-I-d. **c** Higher magnification of the *boxed area* in **b** showing the mineralized tissues on the surface of the TCP particles in the part of the implants cultured on Col-I-d. **d** No specific staining with the BSP antibody was observed in implants of DFC-I cultured on P-d. **e** Specific staining with BSP was clearly observed in the extracellular matrix of the cells lining the TCP particles from DFC-I cultured on Col-I-d. **f** Higher magnification of the *boxed area* in **e** showing specific staining for BSP in the cytoplasm of cells cultured on Col-I-d and on the surface of the TCP particles (*arrowheads*). **g** Implants of DFC-I cultured on P-d showed no positive Von Kossa staining. **h** Von Kossa staining showed clear mineral nodules (*arrow*) in the parts of implants of DFC-I cultured on Col-I-d and on the surface of the TCP particles (*arrowhead*). **i–l** Morphology of representative implants of DFC-I cultured on P-d (**i**, **k**) and Col-I-d (**j**, **l**), at 8 weeks after transplantation. **i** Hard tissue formation was clearly identified. Bone-like tissues were formed, and osteocyte-like cells were embedded in the part of implants of DFC-I cultured on P-d (*asterisk*). **j** The bone-like tissues were clearly visible in the implants from Col-I-d (*asterisk*). **k** Cementum-like tissues were formed and lined the TCP-particle surfaces (*asterisk*) in the part of implants cultured on P-d. **l** Cementum-like tissues were formed and lined the TCP-particle surfaces in the part of the implants from Col-I-d culture (*asterisk*). No clear differences were apparent in the amount of hard tissue formation in the implants from DFC-I cultured on Col-I-d compared with P-d. *Bars* 200 μm (**a**, **b**, **d**, **e**, **g**, **h**), 100 μm (**c**, **f**, **i**, **j**, **k**, **l**)

in PDLC. These results demonstrated that gene expression patterns in DFC-I cultured on Col-I resembled those of PDLC.

Developmental potential of clone-DFC-I in vivo

In vivo characterization of clone-DFC-I

To extend the comparison of DFC-I cultured on Col-I-d and on P-d, we investigated the potential for mineralization in vivo by transplanting DFC-I in conjunction with TCP into the subcutaneous tissue of immunocompromised scid mice as described previously (Handa et al. 2002; Saito et al. 2005). At 1, 2, and 4 weeks after transplantation, we examined the relevant gene expression in the implants by sq-PCR. No expression of the BSP or periostin genes was seen at 1 week after transplantation in either implant type (DFC-I cultured on Col-I-d versus P-d), but clear expression was detected at 2 and 4 weeks (Fig. 6a,b). Periostin expression was distinctly lower in Col-I-d-cultured implants than in P-d-cultured implants (Fig. 6a,e). OCN and OPN expression was strongly detected in both implants at 4 weeks, with higher levels being detected in the Col-I-d-cultured implants than in those cultured on P-d (Fig. 6a,c,d). Collagen type III expression in implants from both dish types was just detectable at 1 week and gradually increased at 2 and 4 weeks, with no differences in expression levels between culturing conditions (Fig. 6a,f).

In vivo histochemical analysis

At 4 weeks, no hard tissue was apparent in control implants (Fig. 7a), but a small amount of calcified tissue was observed in the experimental group (Fig. 7b,c). We therefore performed immunohistochemical staining on the complex of TCP and developing DFC to examine this possibility in more detail. Some of the cells lining the TCP particles were positive for BSP antibody staining in the experimental group (Fig. 7e,f), whereas no positive staining was detected in the control group (Fig. 7d). Furthermore, Von Kossa staining was performed to investigate whether DFC-I cells cultivated on Col-I-d would promote the formation of mineralized nodules. This staining revealed substantial mineralization of tissue in the implants with DFC-I cultivated on Col-I-d (Fig. 7h), but not in the implants with DFC-I cultivated on P-d (Fig. 7g). These results indicated that DFC-I under Col-I culture conditions had an advanced ability to induce hard tissue formation.

At 8 weeks, hard tissues were identified in both implants on the surface of TCP particles and in the cells (Fig. 7i–l), with no obvious difference between the two experimental groups.

Discussion

We have obtained one clonal cell population (DFC-I) from porcine cultured DFC isolated from developing teeth at the early crown-formation stage. Although previous studies have analyzed DFC from the root surface during root formation, no data exist for cells at the early crown-formation stage (Hakki et al. 2001; Handa et al. 2002; Jin et al. 2003; Saito et al. 2005). The isolation of progenitor cells from the DF may therefore help to identify the as-yet-unknown mechanism for differentiation into the cementoblasts, PDL fibroblasts, and osteoblasts that make up the periodontium (Lekic et al. 1996; Pitaru et al. 1994). The properties exhibited by a single cell clone population could possibly be used to elucidate the mechanisms of differentiation. Based on these ideas, we have propagated and characterized DFC-I with respect to the expression of several marker genes preferentially expressed in PDLC and BMSC (Table 1).

Characterization of the DFC-I gene expression pattern has revealed inconsistencies from the patterns among DF, nonclone-DFC, PDLC, and BMSC. Comparison of our DFC-I with PDLC and BMSC has shown that most osteogenesis-related genes including BSP, OPN, and CTGF are not detectable in DFC-I, although BSP, OPN, and CTGF have been detected in DF and BMSC. Normally, OPN is expressed followed first by BSP and subsequently by OCN, which characterizes the postproliferative phase (Aubin 2001; Liu et al. 2003). Biglycan is a small leucine-rich proteoglycan that binds to various ECM components and has a role in mineralization (Xu et al. 1998). With regard to PDLC, no clear differentiation marker specifically characterizes this type of cell, especially in the pig. In this study, periostin expression has been weakly detected in DFC-I, but strongly in PDLC. Taken together, our results demonstrate the low expression of genes related to osteogenesis in the DFC-I, despite the ECM being osteogenic at this stage of development. Although the DF consists of heterogeneous cell populations, our findings suggest that DFC-I is an immature cell type, distinct from both PDLC and BMSC. Recently, three types of DFC have been reported (Luan et al. 2006). Further examination of the other clone-cell populations obtained in the present study from one tooth bud at the early crown-formation stage is therefore required.

As a second aim of this study, we have evaluated the effect of a Col-I matrix on DFC-I. Col-I is well known to interact with $\alpha1\beta1$, $\alpha2\beta1$, and $\alpha3\beta1$ integrin receptors via the DGEA amino acid sequence (Staatz et al. 1991). A previous study has demonstrated that Col-I regulates OCN gene expression, and the mRNA level of OCN gene expression is upregulated in dental pulp cells (Mizuno et al. 2003). By immunohistochemistry, we have shown that

Col-I is a major component of the DF. We have further shown that ALPase activity is higher in Col-I-treated DFC-I, suggesting a role for Col-I in stimulating the differentiation of DFC-I. Sasaki et al. (1990) have shown intense ALPase activity along the plasma membranes of whole cell surfaces in cementoblasts of human deciduous teeth. Moreover, PDLC also express high ALPase activity (Giannopoulou and Cimasoni 1996; Ogata et al. 1995) in vitro in the presence of osteogenic medium (Nohutcu et al. 1997; Ramakrishnan et al. 1995). These findings are in agreement with our results.

We have further explored the expression of genes associated with the periodontium. DFC are similar to odontoblasts and osteoblasts in terms of mineralized tissue formation (Gronthos et al. 2000; Shi et al. 2001). However, the gene expression of BSP has not been found to be upregulated by Col-I in our study. Our results are therefore not consistent with expression patterns in dental pulp and MSCs. On the other hand, Col-I potently stimulates the expression of periostin, biglycan, and OCN in DFC-I. A recent study has shown that PDLC lines and osteoblasts share the expression of gene for periostin but not the genes for BSP or OCN (Saito et al. 2002). Biglycan facilitates the initiation of apatite formation and inhibits the growth of apatite in a gelatin gel system (Boskey et al. 1997). Our results are consistent with these observations and suggest that the expression pattern of DFC-I exposed to Col-I resembles those of PDLC. Together, the results of the ALPase activity and gene expression analyses therefore indicate that a Col-I matrix influences the differentiation of immature DFC along the osteogenic pathway, as for PDLC. However, the limited data obtained from one specific cell population in the present study may be insufficient to provide information on this issue. Therefore, further study is needed on the other clone populations.

Finally, we tested whether DFC-I have the capacity to produce hard tissue. Progenitor cells isolated from bovine DF at the root-formation stage have previously been shown to generate cementum (Handa et al. 2002); however, no data exist for DFC at the early crown-formation stage. Examination of the gene expression patterns related to osteogenesis has revealed the expression of BSP at 2 weeks after transplantation, and OCN, periostin, and collagen type III expressions gradually increase. OCN appears immediately before the start of mineralization (Nakashima 1994), and BSP mRNA is expressed almost exclusively in differentiated osteoblasts, odontoblasts, and cementoblasts (Bianco et al. 1991; Chen et al. 1991b, 1992). Significant differences occur in BSP and periostin expression at 2 and 4 weeks and in OCN at 4 weeks between implants cultured on Col-I-d versus P-d and suggest that Col-I promotes follicle cells in the TCP particles to differentiate along a mineralization pathway in vivo.

The implants in control groups at 4 weeks have no hard tissues, whereas the implants of the experiment group show a small extent of calcification by Von Kossa staining. In addition, a significant difference has been observed in BSP immunostaining. When DFC cultured on Col-I are implanted, the cells lining the TCP particles are BSP-immunostained, but this is not seen with P-d. At 8 weeks, hard tissue formation is apparent in both groups. These findings therefore suggest that the DFC-I under the TCP particles develop into a cementoblast/osteoblast lineage capable of forming a mineralized ECM, and that Col-I facilitates this differentiation in vivo. However, specific factors promoting this differentiation have not been identified in these studies.

Up to now, PDLC have been obtained from the tooth-root surface to establish periodontal-tissue engineering (Akizuki et al. 2005; Hasegawa et al. 2005). Thus, a tooth has to be extracted to obtain periodontal tissues. Most people have an impacted third molar that does not cause occlusion. The DF usually involves impacted third molars, which are often extracted for orthodontic therapy. The use of impacted third molars as a cell source for periodontal-tissue engineering might expand the avenues for treatment of disease in this field. The present DF study may be a promising first step toward complete periodontal-tissue engineering.

Acknowledgments We thank Dr. J. Sodek for generously providing the collagen type I and BSP antibodies (University of Toronto, Canada), Dr. H. Irie for the kind gift of the Osferion G1 (Olympus, Japan), and Dr. A. Kamiya (IMSUT, Japan) for technical support.

References

Akintoye SO, Lam T, Shi S, Brahim J, Collins MT, Robey PG (2006) Skeletal site-specific characterization of orofacial and iliac crest human bone marrow stromal cells in same individuals. Bone 38:758–768

Akizuki T, Oda S, Komaki M, Tsuchioka H, Kawakatsu N, Kikuchi A, Yamato M, Okano T, Ishikawa I (2005) Application of periodontal ligament cell sheet for periodontal regeneration: a pilot study in beagle dogs. J Periodontal Res 40:245–251

Alliot-Licht B, Bluteau G, Magne D, Lopez-Cazaux S, Lieubeau B, Daculsi G, Guicheux J (2005) Dexamethasone stimulates differentiation of odontoblast-like cells in human dental pulp cultures. Cell Tissue Res 321:391–400

Aubin JE (2001) Regulation of osteoblast formation and function. Rev Endocr Metab Disord 2:81–94

Bartold PM, Miki Y, McAllister B, Narayanan AS, Page RC (1988) Glycosaminoglycans of human cementum. J Periodontal Res 23:13–17

Bianco P, Fisher LW, Young MF, Termine JD, Robey PG (1991) Expression of bone sialoprotein (BSP) in developing human tissues. Calcif Tissue Int 49:421–426

Bianco P, Riminucci M, Gronthos S, Robey PG (2001) Bone marrow stromal stem cells: nature, biology, and potential applications. Stem Cells 19:180–192

Boskey AL, Spevak L, Doty SB, Rosenberg L (1997) Effects of bone CS-proteoglycans, DS-decorin, and DS-biglycan on hydroxyapatite formation in a gelatin gel. Calcif Tissue Int 61:298–305

Chen J, Zhang Q, McCulloch CA, Sodek J (1991a) Immunohistochemical localization of bone sialoprotein in foetal porcine bone tissues: comparisons with secreted phosphoprotein 1 (SPP-1, osteopontin) and SPARC (osteonectin). Histochem J 23:281–289

Chen JK, Shapiro HS, Wrana JL, Reimers S, Heersche JN, Sodek J (1991b) Localization of bone sialoprotein (BSP) expression to sites of mineralized tissue formation in fetal rat tissues by in situ hybridization. Matrix 11:133–143

Chen J, Shapiro HS, Sodek J (1992) Development expression of bone sialoprotein mRNA in rat mineralized connective tissues. J Bone Miner Res 7:987–997

Diekwisch TG (2001) The developmental biology of cementum. Int J Dev Biol 45:695–706

Ducy P, Starbuck M, Priemel M, Shen J, Pinero G, Geoffroy V, Amling M, Karsenty G (1999) A Cbfa1-dependent genetic pathway controls bone formation beyond embryonic development. Genes Dev 13:1025–1036

Giannopoulou C, Cimasoni G (1996) Functional characteristics of gingival and periodontal ligament fibroblasts. J Dent Res 75:895–902

Gronthos S, Mankani M, Brahim J, Robey PG, Shi S (2000) Postnatal human dental pulp stem cells (DPSCs) in vitro and in vivo. Proc Natl Acad Sci USA 97:13625–13630

Hakki SS, Berry JE, Somerman MJ (2001) The effect of enamel matrix protein derivative on follicle cells in vitro. J Periodontol 72:679–687

Han X, Amar S (2003) IGF-1 signaling enhances cell survival in periodontal ligament fibroblasts vs. gingival fibroblasts. J Dent Res 82:454–459

Handa K, Saito M, Tsunoda A, Yamauchi M, Hattori S, Sato S, Toyoda M, Teranaka T, Narayanan AS (2002) Progenitor cells from dental follicle are able to form cementum matrix in vivo. Connect Tissue Res 43:406–408

Hasegawa M, Yamato M, Kikuchi A, Okano T, Ishikawa I (2005) Human periodontal ligament cell sheets can regenerate periodontal ligament tissue in an athymic rat model. Tissue Eng 11:469–478

Hsu SM, Raine L, Fanger H (1981) Use of avidin-biotin-peroxidase complex (ABC) in immunoperoxidase techniques: a comparison between ABC and unlabeled antibody (PAP) procedures. J Histochem Cytochem 29:577–580

Iohara K, Nakashima M, Ito M, Ishikawa M, Nakasima A, Akamine A (2004) Dentin regeneration by dental pulp stem cell therapy with recombinant human bone morphogenetic protein 2. J Dent Res 83:590-595

Jin QM, Zhao M, Webb SA, Berry JE, Somerman MJ, Giannobile WV (2003) Cementum engineering with three-dimensional polymer scaffolds. J Biomed Mater Res [A] 67:54–60

Klees RF, Salasznyk RM, Kingsley K, Williams WA, Boskey A, Plopper GE (2005) Laminin-5 induces osteogenic gene expression in human mesenchymal stem cells through an ERK-dependent pathway. Mol Biol Cell 16:881–890

Lekic P, Sodek J, McCulloch CA (1996) Relationship of cellular proliferation to expression of osteopontin and bone sialoprotein in regenerating rat periodontium. Cell Tissue Res 285:491–500

Lekic P, Rojas J, Birek C, Tenenbaum H, McCulloch CA (2001) Phenotypic comparison of periodontal ligament cells in vivo and in vitro. J Periodontal Res 36:71–79

Liu F, Malaval L, Aubin JE (2003) Global amplification polymerase chain reaction reveals novel transitional stages during osteoprogenitor differentiation. J Cell Sci 116:1787–1796

Luan X, Ito Y, Dangaria S, Diekwisch TG (2006) Dental follicle progenitor cell heterogeneity in the developing mouse periodontium. Stem Cells Dev 15:595–608

Marcopoulou CE, Vavouraki HN, Dereka XE, Vrotsos IA (2003) Proliferative effect of growth factors TGF-beta1, PDGF-BB and rhBMP-2 on human gingival fibroblasts and periodontal ligament cells. J Int Acad Periodontol 5:63–70

Mizuno M, Kuboki Y (2001) Osteoblast-related gene expression of bone marrow cells during the osteoblastic differentiation induced by type I collagen. J Biochem (Tokyo) 129:133–138

Mizuno M, Miyamoto T, Wada K, Watatani S, Zhang GX (2003) Type I collagen regulated dentin matrix protein-1 (Dmp-1) and osteocalcin (OCN) gene expression of rat dental pulp cells. J Cell Biochem 88:1112–1119

Morsczeck C, Gotz W, Schierholz J, Zeilhofer F, Kuhn U, Mohl C, Sippel C, Hoffmann KH (2005) Isolation of precursor cells (PCs) from human dental follicle of wisdom teeth. Matrix Biol 24:155–165

Murakami Y, Kojima T, Nagasawa T, Kobayashi H, Ishikawa I (2003) Novel isolation of alkaline phosphatase-positive subpopulation from periodontal ligament fibroblasts. J Periodontol 74:780–786

Nakao K, Itoh M, Tomita Y, Tomooka Y, Tsuji T (2004) FGF-2 potently induces both proliferation and DSP expression in collagen type I gel cultures of adult incisor immature pulp cells. Biochem Biophys Res Commun 325:1052–1059

Nakashima M (1994) Induction of dentin formation on canine amputated pulp by recombinant human bone morphogenetic proteins (BMP)-2 and -4. J Dent Res 73:1515–1522

Nohutcu RM, McCauley LK, Koh AJ, Somerman MJ (1997) Expression of extracellular matrix proteins in human periodontal ligament cells during mineralization in vitro. J Periodontol 68: 320–327

Ogata Y, Niisato N, Sakurai T, Furuyama S, Sugiya H (1995) Comparison of the characteristics of human gingival fibroblasts and periodontal ligament cells. J Periodontol 66:1025–1031

Ouyang H, McCauley LK, Berry JE, D'Errico JA, Strayhorn CL, Somerman MJ (2000) Response of immortalized murine cementoblasts/periodontal ligament cells to parathyroid hormone and parathyroid hormone-related protein in vitro. Arch Oral Biol 45: 293–303

Palmer RM, Lumsden AG (1987) Development of periodontal ligament and alveolar bone in homografted recombinations of enamel organs and papillary, pulpal and follicular mesenchyme in the mouse. Arch Oral Biol 32:281–289

Pavasant P, Yongchaitrakul T, Pattamapun K, Arksornnukit M (2003) The synergistic effect of TGF-beta and 1,25-dihydroxyvitamin D3 on SPARC synthesis and alkaline phosphatase activity in human pulp fibroblasts. Arch Oral Biol 48:717–722

Piattelli A, Trisi P, Passi P, Piattelli M, Cordioli GP (1994) Histochemical and confocal laser scanning microscopy study of the bone-titanium interface: an experimental study in rabbits. Biomaterials 15:194–200

Pitaru S, McCulloch CA, Narayanan SA (1994) Cellular origins and differentiation control mechanisms during periodontal development and wound healing. J Periodontal Res 29:81–94

Pitaru S, Pritzki A, Bar-Kana I, Grosskopf A, Savion N, Narayanan AS (2002) Bone morphogenetic protein 2 induces the expression of cementum attachment protein in human periodontal ligament clones. Connect Tissue Res 43:257–264

Ramakrishnan PR, Lin WL, Sodek J, Cho MI (1995) Synthesis of noncollagenous extracellular matrix proteins during development of mineralized nodules by rat periodontal ligament cells in vitro. Calcif Tissue Int 57:52–59

Ruch JV (1998) Odontoblast commitment and differentiation. Biochem Cell Biol 76:923–938

Saito Y, Yoshizawa T, Takizawa F, Ikegame M, Ishibashi O, Okuda K, Hara K, Ishibashi K, Obinata M, Kawashima H (2002) A cell line with characteristics of the periodontal ligament fibroblasts is negatively regulated for mineralization and Runx2/Cbfa1/Osf2

activity, part of which can be overcome by bone morphogenetic protein-2. J Cell Sci 115:4191–4200

Saito M, Handa K, Kiyono T, Hattori S, Yokoi T, Tsubakimoto T, Harada H, Noguchi T, Toyoda M, Sato S, Teranaka T (2005) Immortalization of cementoblast progenitor cells with Bmi-1 and TERT. J Bone Miner Res 20:50–57

Salasznyk RM, Williams WA, Boskey A, Batorsky A, Plopper GE (2004) Adhesion to vitronectin and collagen I promotes osteogenic differentiation of human mesenchymal stem cells. J Biomed Biotechnol 2004:24–34

Sasaki T, Watanabe C, Shimizu T, Debari K, Segawa K (1990) Possible role of cementoblasts in the resorbant organ of human deciduous teeth during root resorption. J Periodontal Res 25:143–151

Saygin NE, Giannobile WV, Somerman MJ (2000) Molecular and cell biology of cementum. Periodontology 24:73–98

Shi S, Robey PG, Gronthos S (2001) Comparison of human dental pulp and bone marrow stromal stem cells by cDNA microarray analysis. Bone 29:532–539

Staatz WD, Fok KF, Zutter MM, Adams SP, Rodriguez BA, Santoro SA (1991) Identification of a tetrapeptide recognition sequence for the alpha 2 beta 1 integrin in collagen. J Biol Chem 266:7363–7367

Ten Cate AR, Mills C (1972) The development of the periodontium: the origin of alveolar bone. Anat Rec 173:69–77

Ten Cate AR, Mills C, Solomon G (1971) The development of the periodontium. A transplantation and autoradiographic study. Anat Rec 170:365–379

Thesleff I, Mikkola M (2002) The role of growth factors in tooth development. Int Rev Cytol 217:93–135

Wise GE, Lin F, Fan W (1992) Culture and characterization of dental follicle cells from rat molars. Cell Tissue Res 267:483–492

Xiao G, Wang D, Benson MD, Karsenty G, Franceschi RT (1998) Role of the alpha2-integrin in osteoblast-specific gene expression and activation of the Osf2 transcription factor. J Biol Chem 273: 32988–32994

Xu T, Bianco P, Fisher LW, Longenecker G, Smith E, Goldstein S, Bonadio J, Boskey A, Heegaard AM, Sommer B, Satomura K, Dominguez P, Zhao C, Kulkarni AB, Robey PG, Young MF (1998) Targeted disruption of the biglycan gene leads to an osteoporosis-like phenotype in mice. Nat Genet 20:78–82

Yoshikawa DK, Kollar EJ (1981) Recombination experiments on the odontogenic roles of mouse dental papilla and dental sac tissues in ocular grafts. Arch Oral Biol 26:303–307

Cell Tissue Res (2008) 331:461–472
DOI 10.1007/s00441-007-0528-x

REGULAR ARTICLE

Characteristic phenotype of immortalized periodontal cells isolated from a Marfan syndrome type I patient

Momotoshi Shiga · Masahiro Saito · Mitsu Hattori · Chiharu Torii · Kenjiro Kosaki · Tohru Kiyono · Naoto Suda

Received: 17 May 2007 / Accepted: 20 September 2007 / Published online: 30 November 2007

Abstract The periodontal ligament (PDL) is situated between the tooth root and alveolar bone, thereby supporting the tooth, and is composed of collagen and elastic system fibers. Marfan syndrome type I (MFS1, MIM #154700) is caused by mutations in *FBN1* encoding fibrillin-1, which is a major microfibrillar protein of elastic system fibers. MFS1 is characterized by tall stature, aortic/mitral valve prolapse, and ectopia lentis and is occasionally accompanied by severe periodontitis. Since little is known about the biological functions of elastic system fibers in PDLs and the pathogenesis of the periodontitis in MFS1, PDL cells were isolated from an MFS1 patient with a heterozygous missense mutation in a calcium-binding epidermal-growth-factor-like domain of *FBN1*. Isolated PDL cells were immortalized by transducing a retrovirus carrying genes for the human Polycomb group protein, Bmi-1, and human telomerase reverse transcriptase. Immortalized PDL cells from the MFS1 patient (termed M-HPL1) and those of a healthy volunteer (termed HPDL2) both expressed various PDL-related genes. The growth and attachment of M-HPL1 and HPDL2 to hydroxyapatite particles were comparable. However, when M-HPL1 were transplanted with hydroxyapatite particles into immunodeficient mice, disorganized cell alignment and irregular microfibril assembly were noted. The activation of the signaling of transforming grwoth factor-β (TGF-β) is thought to cause the pathogenesis for lung and cardiovascular abnormalities in MFS1. Interestingly, M-HPL1 shows a higher level of activated TGF-β than HPDL2. Thus, M-HPL1 represent a powerful tool for clarifying the biological roles of elastic system fibers in PDL and the pathogenesis of periodontitis in MFS1. Our findings also suggest that *FBN1* regulates cell alignment and microfibril assembly in PDLs.

Keywords Elastic fiber · Fibrillin-1 · Marfan syndrome · Periodontitis · Periodontal ligament · Human

This work was supported by Grants-in-Aid (16390604, 16659570, and 18390552) for Scientific Research from the Ministry of Education, Culture, Sports, Science, and Technology of Japan.

M. Shiga · M. Hattori · N. Suda (✉)
Maxillofacial Orthognathics, Department of Maxillofacial Reconstruction and Function,
Division of Maxillofacial/Neck Reconstruction, Graduate School,
Tokyo Medical and Dental University,
1-5-45 Yushima, Bunkyo-ku,
Tokyo 113-8549, Japan
e-mail: n-suda.mort@tmd.ac.jp

M. Saito
Department of Molecular and Cellular Biochemistry,
Graduate School of Dentistry, Osaka University,
Osaka 565-0871, Japan

C. Torii · K. Kosaki
Department of Pediatrics, Keio University School of Medicine,
Tokyo 160-8582, Japan

T. Kiyono
Virology Division, National Cancer Center Research Institute,
Tokyo 104-0045, Japan

Introduction

The periodontal ligament (PDL) is a specialized connective tissue situated between the cementum covering the root of teeth and the alveolar bone socket (Beertsen et al. 1997; Freeman 1998). PDLs consist of various kinds of cells and fibers. The cells include fibroblasts, epithelial cell remnants of Malassez, macrophages, undifferentiated mesenchymal cells, cementoblasts, osteoblasts, and osteoclasts. The fibers include collagen and elastic system fibers. PDLs are well adapted to support teeth in bone and to act as a sensory

receptor. To support teeth, collagen fibers are embedded both in the cementum and alveolar bone, and each collagen fiber works as a spliced rope to withstand the considerable forces of mastication.

Elastic system fibers provide elasticity and resistance to stretch and expansion forces (Mecham 1991). They are widely distributed in various tissues, e.g., skin, lungs, eyes, and blood vessels. Three types of elastic system fibers (oxytalan and elastic and elaunin fibers) are known; they differ in the content of elastin (Kielty et al. 2002). Oxytalan fibers solely consist of bundles of microfibrils, which are predominantly composed of glycoproteins and fibrillin-1 and -2. The elastic fibers are constructed of bundles of microfibrils peripherally associated with elastin. In the elaunin fibers, bundles of microfibrils are intermingled with small amounts of elastin. In the PDL, the main elastic system fibers are oxytalan fibers oriented in an occluso-apical direction (Fullmer et al. 1974; Beertsen et al. 1997). A small amount of elaunin fibers is also found in the apical region (Staszyk and Gasse 2004; Sawada et al. 2006). In contrast to collagen fibers, the biological functions of the elastic system fibers in PDLs are still obscure.

Marfan syndrome type I (MFS1, MIM #154700) is an autosomal dominant disorder affecting the elastic system fibers. Its prevalence has been estimated to be 2–3 per 10,000 (Nollen and Mulder 2004). MFS1 is characterized by various clinical manifestations primarily in skeletal, ocular, and cardiovascular organs, e.g., tall stature, aortic dissection, mitral valve prolapse, and ectopia lentis (Pyeritz 2000). The responsible gene for this syndrome has been identified as *FBN1*, which encodes the major microfibrillar protein, fibrillin-1 (Dietz et al. 1991; Maslen et al. 1991). In addition to anomalies in skeletal, ocular, and cardiovascular systems, MFS1 exhibits characteristic oral features including maxillary protrusion (Westling et al. 1998), high palate, and crowding and fragility of the temporomandibular joint (Bauss et al. 2004). Severe periodontitis, which has a serious impact on the quality of life of MFS1 patients, is occasionally associated with this syndrome (Straub et al. 2002).

To clarify the biological functions of fibrillin-1 in PDLs and the pathogenesis of the periodontitis in MFS1, PDL cells have been isolated from an MFS1 patient. The prepared immortalized PDL cells, which have a mutation in a calcium-binding epidermal-growth-factor-like (cbEGF) domain of fibrillin-1, might be a powerful tool to help answer these questions.

Materials and methods

Subjects

The patient was a 46-year-old female. She was 172 cm tall, weighed 58 kg, and had arachnodactyly. Her father and younger brother were also diagnosed as having Marfan syndrome. She had previously had dissecting aneurysm of the aorta and had had a surgical replacement of the aortic root (Bentall operation) at 42 years of age. She had suffered from mitral valve prolapse and had had a replacement of the mitral valve at 46 years of age. Since she had severe periodontitis in all teeth, all teeth were extracted before the mitral valve replacement to avoid infective endocarditis. The patient kindly provided these teeth to us with consent.

Extracted teeth were also provided by three healthy volunteers (volunteer A, 15-year-old male; volunteer B, 15-year-old male; volunteer C, 21-year-old female) during the course of orthodontic treatment, with consent. The experimental protocol was approved by the Ethical Review Committee of Tokyo Medical and Dental University.

Isolation and culture of primary PDL cells

Isolation and culture of human PDL cells were performed as previously described (Kapila et al. 1996; Shiga et al. 2003). In brief, the extracted teeth from the MFS1 patient and healthy volunteers were washed with α-minimum essential medium (α–MEM; Kohojin Bio, Japan) containing Antibiotic-Antimycotic (GIBCO, Calif.). The PDL attached to the middle part of the root was isolated with a surgical scalpel. The PDL was minced and placed in 35-mm tissue culture dishes (SUMILON, Japan). The explants were then covered with sterile glass coverslips and incubated in α–MEM with 10% fetal bovine serum (FBS; Japan Bioserum, Japan) at 37°C under 5% CO_2 and 95% air until cells outgrew from the explants. After the outgrowth of cells, coverslips were removed from the culture dishes. The culture medium was changed every 3 days. PDL cells from passages 3–7 were used for examing mineralization, measuring alkaline phosphatase (ALP) activity, and transduction.

Mineralization of the primary culture of PDL cells

To determine the mineralization of cultured PDL cells, cells were plated at 2.0×10^4 cells/cm^2 and cultured in α–MEM containing 10% FBS. After cells became confluent, the medium was changed to α–MEM containing 10% FBS with 50 μg/ml ascorbic acid (Wako, Japan), 10 nM dexamethasone (Sigma, Mo.), and 10 mM β-glycerophosphate (Sigma) in some cultures, as previously described (Cho et al. 1992; Nohutcu et al. 1997; Chien et al. 1999). The medium was changed every 3 days, and the cells were cultured for 3 weeks. Mineralized matrix in the culture were stained by Alizarin Red S (Wako, Japan) at the end of the culture (Saito et al. 2002). All experiments were performed in triplicate wells.

ALP activity

Cells were cultured under the same conditions as described above for mineralization. ALP activity was assayed in cell lysates by enzymatic conversion of the p-nitrophenylphosphate substrate to p-nitrophenol by using the LabAssay ALP kit (Wako) according to the manufacturer's instructions. The activity was recorded as millimoles per milligram per 15 min. The total protein amount in the cell lysates was measured by using the Bradford microassay (Bio-Rad, Calif.) according to the manufacturer's instructions.

Immunohistochemical staining of cultured PDL cells

Cultured PDL cells were immunohistochemically stained by using anti-human periostin rabbit polyclonal antibody (BioVendor laboratory Medicine, N.C.), anti-bovine collagen type XII monoclonal antibody (Clone 378D5, Kamiya Biomedical, Wash.), anti-active transforming growth factor-β (TGF-β) rabbit polyclonal antibody (LC1-30, provided by K. Flanders, National Cancer Institute, Md.; Flanders et al. 1989), or anti-human latency-associated peptide-β1 (LAP-β1) goat polyclonal antibody (R&D systems, Minn.). Cells (2.0×10^4 cells/cm^2) were cultured on poly-L-lysine-coated glass (Iwaki, Japan). They were then fixed with 4% paraformaldehyde (PFA) for 30 min, blocked with 1% bovine serum albumin (BSA), and incubated with each antibody for 1 h. Sections were then treated with Alexa Fluor 594 goat anti-rabbit IG (H+L; Invitrogen, Calif.), Alexa Fluor 488 goat anti-mouse IG (H+L; Invitrogen), or Alexa Fluor 488 donkey anti-goat IG (H+L; Invitrogen). As negative controls, primary antibodies were replaced with normal rabbit serum (Vector Laboratories, Calif.), mouse IgG (Jackson Immuno Research Laboratories, Pa.), or normal goat serum (Vector Laboratories). After washes with phosphate-buffered saline, fluorescence was observed by means of a fluorescence microscope (AF6000, Leica, Germany).

Mutational analysis

DNA from the MFS1 patient and healthy volunteers was extracted by using a DNA extraction kit (Bio-Rad, Calif.). Extracted DNA was amplified by using specific primers for *FBN1* and *TGFBR2* (encoding TGF-β receptor II, which is the responsible gene for Marfan syndrome type II; MFS2, MIM #154705; Mizuguchi et al. 2004). Primer sequences and polymerase chain reaction (PCR) conditions were as given on the website of "Multiple Malformation Syndromes (http://www.dhplc.jp/genetics/frame.html)" provided by the Department of Pediatrics, Division of Medical Genetics, Keio University School of Medicine. Mutations in each amplicon were analyzed by denaturing high-performance liquid chromatography (DHPLC), as described in previous studies (Kosaki et al. 2005; Udaka et al. 2005).

After DHPLC analysis, PCR products were purified on a desalting column and were sequenced by a dideoxy-sequencing method (BigDye Dideoxy sequencing kit, Applied BioSystems, Calif.) and an automated sequencer (ABI3100, Applied Biosystems; Udaka et al. 2005).

Retroviral vectors and infection

Primary PDL cells, obtained from a healthy volunteer and the MFS1 patient, were transduced with genes for human Polycomb group protein, Bmi-1, and human telomerase reverse transcriptase (hTERT) by using retrovirus-mediated gene transfer. The production and infection of LXSN-Bmi-1 and MSCVpuro-hTERT retroviruses were performed as described previously (Kyo et al. 2003; Saito et al. 2005). The infected cells were selected in the presence of geneticin (125 μg/ml) or puromycin (0.5 μg/ml). For combined retroviral infection, cells were sequentially transduced with LXSN-Bmi-1 and then with MSCVpuro-hTERT. Stably transduced cells were maintained in the medium described above.

Detection of telomerase activity

After infection, telomerase activity was determined by a telomerase repeat amplification assay by using the TRA-Peze Telomerase Detection Kit (CHEMICON International, Calif.), according to the manufacturer's instructions.

Cell proliferation in monolayer culture

To examine cell proliferation, cells were inoculated at 5.0×10^3 cells/cm^2 into 6-well dishes (Iwaki, Japan) and cultured in α–MEM containing 10% FBS. The medium was changed every 3 days, and cells were counted every 3 days up to day 15. All experiments were performed in triplicate wells.

Western blot analysis

The introduction of Bmi-1 was identified by Western blot analysis by using anti-human Bmi-1 monoclonal antibody (BD Pharmingen, San Diego, Calif.). Cells were cultured in α–MEM containing 10% FBS and lysed in buffer containing 50 mM TRIS-HCl (pH 7.4), 125 mM NaCl, 0.1% Nonident P-40 (NP-40; Sigma), and 1 mM each of EDTA and phenylmethylsulfonyl fluoride, followed by sonication. After electrophoretic resolution of the cell lysate (20 μg each protein) on 12.5% SDS-polyacrylamide gels, the proteins were transferred to polyvinylidene difluoride (PVDF) membranes (Amersham, N.J.). The subsequent

detection procedure was performed as described previously (Saito et al. 2005).

RNA preparation and reverse transcription/PCR

Total RNA was isolated from primary PDL cells (both from healthy volunteer B and the MFS1 patient) and from immortalized PDL cells cultured in α–MEM containing 10% FBS, by using ISOGEN (Nippon Gene, Japan) according to the manufacturer's instructions. cDNA was synthesized from 1 μg total RNA by QuantiTect Reverse Transcription (QIAGEN, Germany), and each cDNA was used as the template for subsequent PCR amplification. Amplification was performed in a GeneAmp PCR System 9700 (Applied Biosystems). The reaction conditions were 94°C for 1 min, 60°C for 30 s, and 72°C for 30 s. The sequences of the used primers were: *POSTN* encoding periostin, sense 5′-ATTGATGGAGTGCCTGTG-3′, antisense 5′-CCTTGGTGACCTCTTCTTG-3′; *ASPN* encoding asporin, sense 5′-CGATACAAAGAACTACAAAGGCT GG-3′, antisense 5′-GCATTTCCCAGTATTTCA CCG-3′; *COL12A1* encoding collagen type XII, sense 5′-CGGA CAGAGCCTTA CGTGCC-3′, antisense 5′-CTGCCC GGGTCCGTGG-3′; *BGLAP* encoding osteoclacin, sense 5′-CCTTTGTGTCCAAGCAGGAG-3′, antisense 5′-TCA GCCAACTCGTCACAGTC-3′; *OPN* encoding osteopontin, sense 5′-TTGCAGTGATTTGCTTTTGC-3′, antisense 5′-TGTGGGG CTAGGAGATTCTG-3′; *BSP* encoding bone sialoprotein, sense 5′-GAACCACTTCCCCACCT TTT-3′, antisense 5′-TCTGACCATCATAGCCATCG-3′; *COL1A1* encoding collagen type I, sense 5′-CTGACCTT CCTGCGCCTGATGTCC-3′, antisense 5′-GTCTGGGGC ACCAACGTCCAAGGG -3′; and a human gene encoding β-actin, sense 5′-ATGAGGATCCTCACCGAGCGCGGCT ACAG C-3′, antisense 5′-ACACCACTGTGTTGGCGTAC AGGTCTTTGC-3′. Optimization of PCR cycle number to allow semi-quantitative analysis was performed by generating saturation curves of amplified product against cycle number. Saturation was seen with 33, 34, 31, 34, 41, 41, 25, and 25 cycles for *POSTN*, *ASPN*, *COL12A1*, *BGLAP*, *OPN*, *BSP*, *COL1A*, and β-actin, respectively. Thus, the semi-quantitative gene expression analysis by reverse transcription/PCR (RT-PCR) was performed with 30, 31, 28, 31, 39, 39, 23, and 23 cycles for *POSTN*, *ASPN*, *COL12A1*, *BGLAP*, *OPN*, *BSP*, *COL1A*, and β-actin, respectively.

A 151-bp fragment of *POSTN* (2220–2370 in NM_006475), a 292-bp fragment of *ASPN* (1031–1322 in NM_017680) (Yamada et al. 2001), a 180-bp fragment of *COL12A1* (7041–7220 in NM_080645), a 151-bp fragment of *BGLAP* (122–272 in NM_199173), a 166-bp fragment of *OPN* (173–338 in NM_001040058), a 201-bp fragment of *BSP* (876–1076 in NM_004967), a 300-bp fragment of *COL1A1* (4180–4479 in NM_000088), and a 327-bp fragment of the gene encoding β-actin (641–967 in NM_001101) were separated on 2% agarose gels (Nippon Gene, Japan) by electrophoresis. The gels were stained with ethidium bromide, photographed under ultraviolet excitation, and analyzed by using picture-imaging software (Scion Image, Scion, Md.).

Cell adhesion assay

To examine the adhesion of PDL cells, viz., HPDL2 from healthy volunteer 2 and M-HPL1 from the MFS1 patient, to hydroxyapatite particles (size 300–500 μm; OSferion, Olympus, Japan), both types of cells were labeled by using the PKH26 Red Fluorescent Cell Linker Mini Kit (Sigma) and incubated with hydroxyapatite particles for 18 h in α–MEM containing 10% FBS. The attached cells were observed by using a fluorescence microscope (AF6000, Leica, Germany).

In vivo differentiation assay

Fiber formation in the HPDL2 and M-HPL1 cells was assessed as described previously (Handa et al. 2002; Saito et al. 2005; Yokoi et al. 2007). Briefly, 1.5×10^6 cells were incubated with 40 mg hydroxyapatite particles and fibrin clot (mixture of mouse fibrinogen and thrombin; Sigma). They were transplanted subcutaneously into 5-week-old male CB-17 *SCID/SCID* mice (Nihon Crea, Japan). Mice were sacrificed after 4 weeks and implanted tissues were collected. Three transplants were prepared for each group, and experiments were repeated in triplicate.

To examine human (not mouse) vimentin-positive cells in transplanted tissues, tissues were fixed in 4% PFA for 1 day, decalcified with 10% formic acid for 3 days, and embedded in paraffin, and 5-μm-thick sections were prepared. To avoid non-specific staining by mouse monoclonal antibodies, sections were blocked by using the M.O.M. kit (Vector Laboratories, Calif.) as previously described (Handa et al. 2002). Sections were incubated, for 1 h, with anti-human vimentin monoclonal antibody (V9, DAKO, Calif.), which recognizes human but not mouse cells. After being washed, sections were incubated with biotinylated secondary antibody (M.O.M. kit) and avidin-peroxidase conjugate (M.O.M. kit). The reaction was visualized by using diaminobenzidine.

To examine human fibrillin-1-positive cells, transplanted tissues were embedded in carboxymethyl cellulose compound (Finetec, Japan), and 5-μm-thick frozen sections were prepared (Kawamoto and Shimizu 2000). Frozen sections were incubated with anti-human fibrillin-1 rabbit polyclonal antibody (Elastin Products, Mo.) for 1 h. After being washed, sections were incubated with Alexa Fluor 594 goat anti-rabbit IG (H+L; Invitrogen), and fluorescence

was observed with a fluorescence microscope (AF6000, Leica, Germany).

Statistical analysis

Student's *t*-test was used to analyze differences in cell numbers between M-HPL1 and HPDL2. Each difference was considered significant at a *P*-value of less than 0.05.

Results

MFS1 patient with a heterozygous mutation in cbEGF domain of FBN1

As shown in Fig. 1a–d, the 46-year-old female patient had severe periodontitis. All teeth had to be extracted before the surgical replacement of the mitral valve to avoid infective endocarditis. Mutational analysis of *FBN1* and *TGFBR2* was performed by using a genomic DNA sample. Since *FBN1* and *TGFBR2* have 65 and 7 exons, respectively, screening of gene mutations before direct sequencing was performed by DHPLC. In total, 65 and 8 amplicons of *FBN1* and *TGFBR2*, respectively, were amplified by PCR and subsequently analyzed by DHPLC. Among them, the peak in the amplicon of exon 52 in *FBN1* from the MFS1 patient shifted to the left compared with that of the wild-type sample (Fig. 1e). This demonstrated heteroduplex formation of the amplicon from the MFS1 patient. Direct sequencing of this product was performed (Fig. 1f). A heterozygous mutation (A to G) was seen at position 6431 (from the translation site in NM_000138). This missense mutation resulted in the replacement of Asn by Ser at amino acid position 2144 (N2144S) in the 32th cbEGF domain (Fig. 1g; see also in previous study of this MFS1 patient in Hewett et al. 1993). Thus, this is not a single nucleotide polymorphism (SNP) or a novel mutation. The elution profile of DHPLC for *TGFBR2* did not show differences between the wild-type sample and MFS1 patient.

Phenotype of primary PDL cells with N2144S mutation from MFS1 patient

Cells were isolated from the PDL of extracted teeth from the MFS1 patient and were cultured in vitro. In order to examine the cellular phenotype of these isolated PDL cells, ALP activity (Fig. 2a) and mineralization (Fig. 2b) were examined. In the cell differentiation medium containing

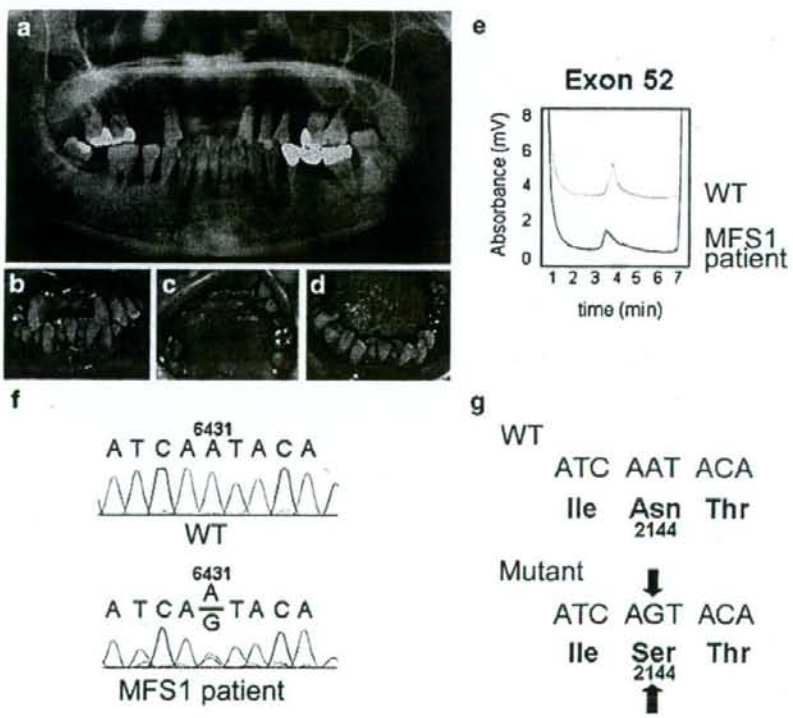

Fig. 1 Severe periodontitis and mutational analysis of the MFS1 patient. **a** In the panoramic X-ray, severe alveolar bone loss was observed around tooth roots. **b–d** Oral photographs showing the severe periodontitis of the patient. **e** DHPLC analysis of exon 52 in *FBN1*. Note the peak in the elution profile of the MFS1 patient shifted to the left compared with that of the wild-type (WT), demonstrating heteroduplex formation. **f** Nucleotide sequence of exon 52 in *FBN1*. **g** Amino acid sequence of fibrillin-1. The 6431A→G change resulted in the heterozygous missense mutation of Asn to Ser (N2144S)

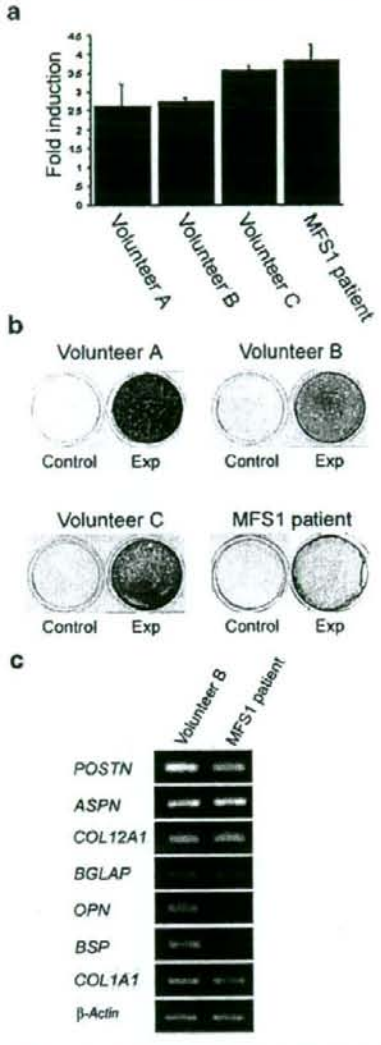

Fig. 2 **a** ALP activities of primary PDL cells isolated from three healthy volunteers (*volunteers A–C*) and the *MFS1 patient*. PDL cells were cultured in the cell differentiation medium containing ascorbic acid (50 μg/ml), β-glycerophosphate (10 mM), and dexamethasone (10 nM) for 3 weeks. Each ALP activity is represented as the ratio (*Fold induction*) to the value before culturing in the cell differentiation medium. PDL cells isolated from the MFS1 patient showed increased ALP activity as in healthy volunteers. **b** Mineralization of PDL cells cultured in the cell differentiation medium for 3 weeks. All PDL cells cultured in the cell differentiation medium were stained positively with Alizarin Red (*Exp*), but were negative when cultured in the medium containing 10% FBS solely (*Control*). **c** Expression of PDL-related genes, such as *POSTN* encoding periostin, *ASPN* encoding asporin, *COL12A1* encoding collagen type XII, *BGLAP* encoding osteocalcin, *OPN* encoding osteopontin, *BSP* encoding bone sialoprotein, *COL1A1* encoding collagen type I, and a human gene encoding β-actin, in cells from volunteer B and the MFS1 patient; reverse transcription/polymerase chain reaction (RT-PCR)

β-glycerophosphate, dexamethasone and ascorbic acid, these cells showed increased ALP activity, as did PDL cells of healthy volunteers (volunteers A–C) after a 3-week culture (Fig. 2a). The PDL cells from the MFS1 patient and healthy volunteers showed mineralization in the cell differentiation medium, but not in the medium only containing 10% FBS (Fig. 2b). The levels of the mineralization varied among cultures. Based on the similarities in the level of mineralization, PDL cells from volunteer B and MFS1 patient were selected for use in the further experiments.

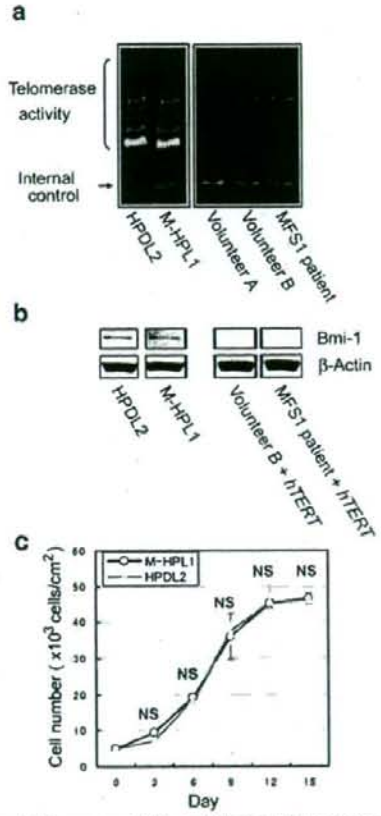

Fig. 3 **a**, **b** Telomerase activity and Western blot analysis of Bmi-1, respectively, in *hTERT*- and *Bmi-1*-transfected HPDL2 (originally from healthy volunteer B) and M-HPL1 (originally from the MFS1 patient). Note the characteristic ladder formation showing telomerase activity in HPDL2 and M-HPL1, but not in untransfected cells (volunteers A or B or MFS1 patient). Western blot analysis showing the expression of Bmi-1 in HPDL2 and M-HPL1, but not in cells transfected solely with *hTERT* (*Volunteer B + hTERT, MFS1 patient + hTERT*). **c** Proliferation of HPDL2 and M-HPL1 in culture. No significant difference occurs in the growth of the two types of cells at days 3, 6, 9, 12, 15 (*NS* not significant). Data represent means ± SD (n=3)

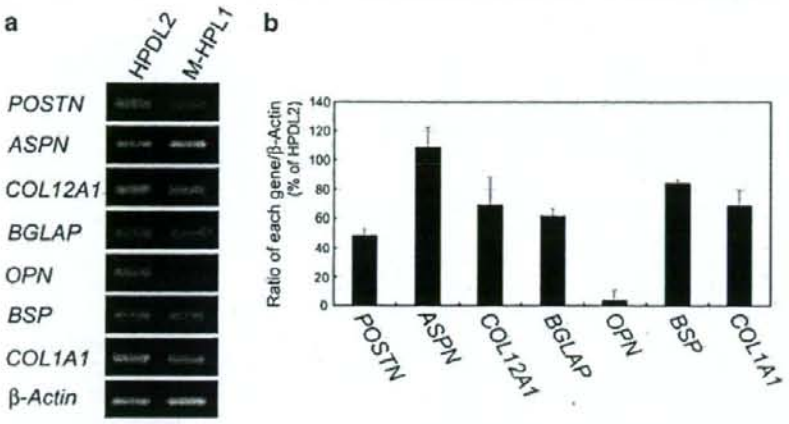

Fig. 4 **a** Expression of *POSTN* encoding periostin, *ASPN* encoding asporin, *COL12A1* encoding collagen type XII, *BGLAP* encoding osteocalcin, *OPN* encoding osteopontin, *BSP* encoding bone sialoprotein, *COL1A1* encoding collagen type I, and a human gene encoding β-actin in immortalized HPDL2 and M-HPL1; RT-PCR. **b** Densitometric data were normalized to β-actin in both types of cells. The bar graph represents the ratios of the expression of each gene in M-HPL1 (% of HPDL2). Data represent means ± SD (n=3)

The expression of various PDL-related genes was examined in cells from volunteer B and MFS1 patient by RT-PCR (Fig. 2c). Both types of PDL cells expressed *POSTN*, *ASPN*, *COL12A1*, *BGLAP*, *BSP*, and *COL1A1*. PDL cells from volunteer B expressed *OPN*. These results demonstrated that, induced by the culture conditions, the isolated PDL cells could differentiate into an osteoblastic phenotype.

Immortalization of isolated PDL cells

Since human cells have a limited life span (Sherr and DePinho 2000), and since the present PDL cells from the MFS1 patient with N2144S are valuable from a research viewpoint, the cultured cells (primary cells from volunteer B and MFS1 patient) were immortalized by retrovirus-mediated transduction. Non-transduced PDL cells and PDL cells transduced solely with *hTERT* showed senescence by passage 15. In contrast, PDL cells transduced with *Bmi-1* and *hTERT* did not show cellular senescence up to passage 20 as indicated by their cell morphology. Thus, we decided to transduce cells with both *Bmi-1* and *hTERT*. The transduced PDL cells from healthy volunteer B and the MFS1 patient were termed HPDL2 and M-HPL1, respectively.

Activation of telomerase by the transduction of *hTERT* was confirmed by the telomerase repeat amplification assay (Fig. 3a). Overexpression of Bmi-1 was confirmed by Western blot analysis (Fig. 3b). Bmi-1 was easily detected in M-HPL1 and HPDL2, but not in cells transduced solely with *hTERT*. No significant difference was seen in the cell growth between HPDL2 and M-HPL1 cultured in medium with 10% FBS up to day 15 (Fig. 3c). After day 12, the cell numbers of neither HPDL2 nor M-HPL1 increased extensively, suggesting that both types of cells had limited proliferation.

Phenotype of HPDL2 and M-HPL1

To characterize the phenotype of the immortalized PDL cells, expression of the reported PDL-related genes and β-actin was examined by semi-quantitative RT-PCR (Fig. 4a). HPDL2 and M-HPL1 both expressed *POSTN*, *ASPN*, *COL12A1*, *BGLAP*, *BSP*, and *COL1A1*. The relative expression of *POSTN*, *COL12A1*, *BGLAP*, and *COL1A1* was lower in M-HPL1 than in HPDL2 (Fig. 4b). *OPN* was expressed in HPDL2, but this was scarcely expressed in M-HPL1 (Fig. 4a, b). Immunohistochemistry with antibodies

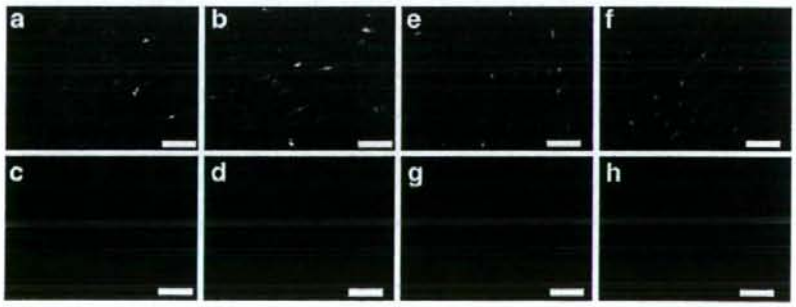

Fig. 5 Positive immunohistochemical localization of collagen type XII in cultured HPDL2 (**a**) and M-HPL1 (**b**) and of periostin in cultured HPDL2 (**e**) and M-HPL1 (**f**). Primary antibodies were replaced with mouse IgG (**c** HPDL2, **d** M-HPL1) or normal rabbit serum (**g** HPDL2, **h** M-HPL1) for negative controls. *Bars* 100 μm

against collagen type XII (Fig. 5a, b) and periostin (Fig. 5e, f) showed numerous immunostained cells in cultures of HPDL2 and M-HDL1. Staining was scarcely seen in negative controls in which primary antibodies had been replaced with mouse IgG (Fig. 5c, d) or normal rabbit serum (Fig. 5g, h).

In the lung (Neptune et al. 2003) and cardiovascular (Ng et al. 2004) systems, gene mutation in *FBN1* has been suggested to be involved in the activation of TGF-β. To examine whether this is the case in M-HPL1, immunostaining with LC1-30, which only recognizes the active form of TGF-β, was performed. M-HPL1 showed more intense staining than HPDL2 (Fig. 6e, f), although a comparable reaction was seen in HPDL2 and M-HPL1 to the antibody against LAP-β1, which also forms complexes with TGF-β (Fig. 6a, b; Miyazono et al. 1993). Staining was scarcely seen in negative controls, in which primary antibodies were replaced with normal goat serum (Fig. 6c, d) or normal rabbit serum (Fig. 6g, h).

Cell and fiber alignments in tissues transplanted with M-HPL1

Ectopic fiber formation by M-HPL1 and HPDL2 in the subcutaneous tissues of SCID mice was examined by transplantation of these cells with hydroxyapatite particles. In this experiment, hydroxyapatite was chosen because it is the major inorganic component of teeth and bones (Ten Cate 1998). HPDL2 (Fig. 7a) and M-HPL1 (Fig. 7b) both attached to the hydroxyapatite particles 18 h after being mixed with the particles.

Four weeks after the transplantation of the cells with hydroxyapatite particles into SCID mice, sections of the cells were immunostained with anti-vimentin antibody recognizing only human but not mouse cells. HPDL2 aligned in parallel between the particles (Fig. 8a, c). In contrast, M-HDL1 were mainly located around the particles and were aligned irregularly (Fig. 8b, d). Similar observations were also seen in eight other transplants from a total of three SCID mice.

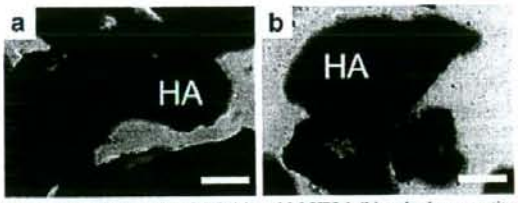

Fig. 7 Attachment of HPDL2 (**a**) and M-HPL1 (**b**) to hydroxyapatite particles (*HA*) after 18-h culture. *Bars* 100 μm

Transplanted tissues were immunostained with anti-human fibrillin-1 antibody. In contrast to the elaborate network of immunoreactive fibrillin-1 in HPDL2, M-HPL1 showed disorganized microfibril assembly (Fig. 9a, b). Staining was scarcely seen in the tissues in which the hydroxyapatite particles without cells were transplanted into SCID mice (Fig. 9c), demonstrating that the antibody only recognized human cells but not mouse cells.

Discussion

The present Japanese female patient had profound skeletal and cardiovascular symptoms including tall stature, arachnodactyly, aortic dissection, mitral valve prolapse, and severe periodontitis. Two types of Marfan syndrome (type I, MIM #154700; type II, MIM #154705) have been described so far. A large French family has been reported to exhibit the skeletal and cardiovascular features of Marfan syndrome in an autosomal dominant manner (Boileau et al. 1993). No mutation in *FBN1* has been seen in this family, and they have been classified as MFS2. Recently, *TGFBR2*

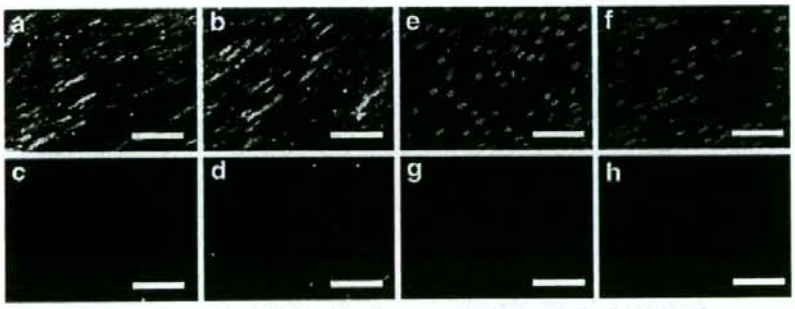

Fig. 6 Immunohistochemical localization of LAP-β1 in cultured HPDL2 (**a**) and M-HPL1 (**b**) and of LCI-30 in cultured HPDL2 (**e**) and M-HPL1 (**f**). Note that LCI-30, which recognizes only the active form of TGF-β, immunoreacts more abundantly in M-HPL1 than in HPDL2, whereas the level of LAP-β1 was comparable in the both types of cells. Primary antibodies were replaced with normal goat serum (**c** HPDL2, **d** M-HPL1) or normal rabbit serum (**g** HPDL2, **h** M-HPL1) for negative controls. *Bars* 100 μm

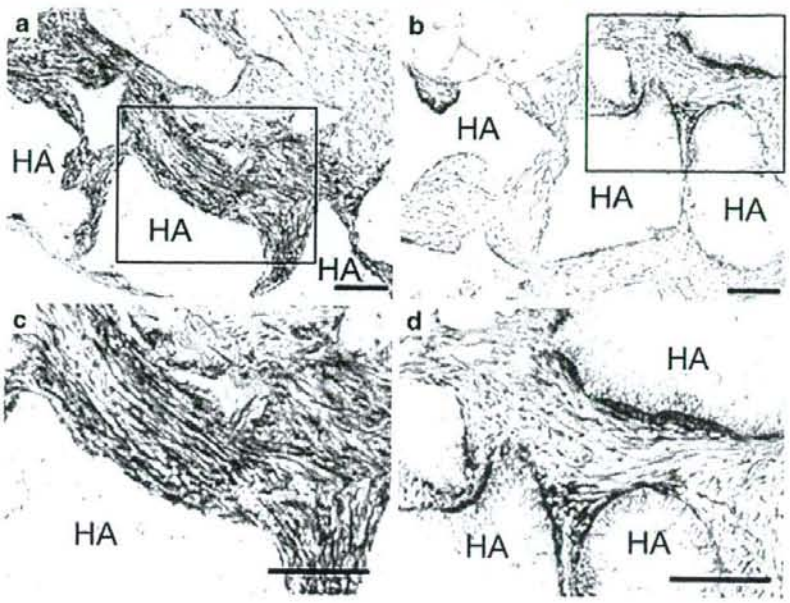

Fig. 8 Sections prepared from tissues in which HPDL2 (**a**, **c**) or M-HPL1 (**b**, **d**) were transplanted with hydroxyapatite particles (*HA*) into SCID mice for 4 weeks. Immunostaining with anti-human vimentin monoclonal antibody. The *boxed areas* in **a**, **b** are shown at higher magnification in **c**, **d**, respectively. Note that HPDL2 aligned in an organized manner, but M-HPL1 showed disorganized alignment. *Bars* 100 μm

has been identified as the responsible gene in MFS2 (Mizuguchi et al. 2004). The present patient has a heterozygous mutation in *FBN1* (Fig. 1f); this mutation results in a missense substitution (N2144S; Fig. 1g), clearly identifying the disease as MFS1.

Since *FBN1* is a large gene with 65 exons, direct sequencing of all the exons to identify mutations is time-consuming and costly. Therefore, we have performed DHPLC to screen for mutations in *FBN1*. In total, 65 amplicons for *FBN1* and 8 amplicons for *TGFBR2* have been synthesized by using specific primers by PCR. Heteroduplex formation has been identified in the product of exon 52 in *FBN1* by DHPLC (Fig. 1e). By using this method, systems have previously been developed to screen 20 congenital disorders (Kosaki et al. 2005). The present DHPLC method is a sensitive and powerful tool that allows the screening of gene mutations before direct sequencing; this is especially useful for large genes such as *FBN1*.

Cells isolated from the PDL of our MFS1 patient and of healthy volunteers have both shown increased ALP activity and mineralization in the cell differentiation medium. PDL cells are known to show an osteoblastic phenotype when cultured under these conditions (Cho et al. 1992; Giannopoulou and Cimasoni 1996; Nohutcu et al. 1997; Chien et al. 1999). After immortalization of cells by introducing *hTERT* and *Bmi-1*, both HPDL2 and M-HPL1 express PDL-related genes, viz., *POSTN* (Fujii et al. 2006), *ASPN* (Yamada et al. 2001), *COL12A1* (Fujii et al. 2006), *BGLAP* (Fujii et al. 2006), *BSP* (Yokoi et al. 2007), and *COL1A1* (Yokoi et al. 2007; Fig. 4a). These observations demonstrate that both types of cells have the characteristic phenotype of cultured PDL cells. However, *POSTN*, *COL12A1*, *BGLAP*, and *COL1A1*

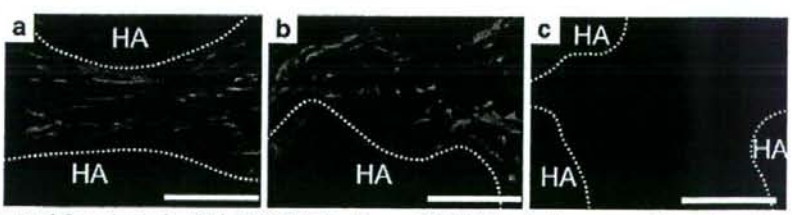

Fig. 9 Sections prepared from tissues in which HPDL2 (**a**) or M-HPL1 (**b**) were transplanted with hydroxyapatite particles (*HA*) into SCID mice for 4 weeks (*dotted lines* outline of HA). Immunostaining with anti-human fibrillin-1 antibody. Note the irregular microfibril assembly in the tissue implanted with M-HPL1 (**b**) but not in that with HPDL2 (**a**). **c** Sections prepared from tissues in which HA particles without cells were transplanted into SCID mice for 4 weeks. Note the absence of immunostaining with anti-human fibrillin-1 antibody (*dotted lines* outline of HA). *Bars* 50 μm

exhibit a lower expression in M-HPL1 than in HPDL2, and *OPN* is hardly expressed in M-HPL1 (Fig. 4a). We now need to examine whether PDL cells isolated from other MFS1 patients reveal a similar down-regulation of these genes.

Recently, attempts have been made to establish immortalized PDL cells by introducing *hTERT* (Berry et al. 2003; Kamata et al. 2004; Fujita et al. 2005; Saito et al. 2005; Fujii et al. 2006; Zhang et al. 2006). Cyclin-dependent kinase inhibitors $p16^{Ink4a}$ and $p21^{WAF1}$ induce premature senescence in human cells by telomere-independent mechanisms (Ramirez et al. 2001). As Bmi-1 can down-regulate the expression of $p16^{Ink4a}$ and $p14^{ARF}$ (Jacobs et al. 1999), it has been used to extend the life span of bovine and human cells (Dimri et al. 2002; Cudre-Mauroux et al. 2003; Itahana et al. 2003; Saito et al. 2005; Haga et al. 2007). Thus, in this study, we have immortalized human PDL cells with retrovirus-mediated transduction of both *hTERT* and *Bmi-1*. By using this method, both HPDL2 and M-HPL1 have been immortalized while maintaining their original gene expressions (Fig. 2c, Fig. 4a), as reported in cementoblast progenitor cells (Saito et al. 2005).

In MFS1, the activation of TGF-β signaling has been suggested as the pathogenesis for mitral valve prolapse and emphysema (Neptune et al. 2003; Ng et al. 2004). Mutations in *FBN1* alter or preclude matrix alteration of the latent complex of TGF-β, rendering TGF-β more accessible for activation (Neptune et al. 2003). In this study, activated TGF-β has been shown to be more abundant in M-HPL1 than in HPDL2 (Fig. 6e, f), suggesting that activated TGF-β signaling occurs in the PDL of our MFS1 patient.

N2144S in fibrillin-1 is predicted to alter one of the key calcium-binding residue ligands within the 32th cbEGF domain (Kettle et al. 1999; Yuan et al. 2002). This mutation is known to increase flexibility in the peptide backbone (Yuan et al. 2002). Attempts should be made to link this mutation and the disorganized cell alignment and microfibril assembly seen in this study.

OPN expression is lower in M-HPL1 than in HPDL2 (Fig. 4a). The exact reason for this difference is not known. However, TGF-β blockade has been reported significantly to enhance the BMP-2-induced upregulation of *OPN* expression, suggesting that TGF-β is a negative regulator on *OPN* expression (Shen et al. 2007). An examination is required of whether decreased expression of *OPN* (Fig. 4a) is mediated by the enhanced TGF-β activation in M-HPL1 (Fig. 6). Moreover, since no study has reported a relationship between fibrillin-1 and *OPN* expression, an investigation of *OPN* expression in M-HPL1 would be of interest after transfecting wild-type fibrillin-1 or during the culture of these cells on the fibrillin-1-coated dishes.

In summary, PDL cells have been isolated from an MFS1 patient with a heterozygous mutation in the 32th cbEGF domain (N2144S). These PDL cells have been immortalized by transducing human *mi-1* and *hTERT*. The present immortalized PDL cells show increased levels of activated TGF-β and should provide a powerful tool for the clarification of the biological roles of the elastic system fibers in PDLs and the pathogenesis of periodontitis in MFS1.

Acknowledgements The authors thank Dr. K. Ohyama (former Professor of Tokyo Medical and Dental University), Dr. S. Yamada (Osaka University), and Professor S. Murakami (Osaka University) for their valuable advice and discussion. The authors are also grateful to Professor T. Yoda (Saitama Medical University) and Dr. Y. Fukushima (Saitama Medical University) for organizing the tooth samples and providing the medical history of the patient. The authors also express their gratitude to Marfan Network Japan (MNJ) for their cooperation in the present research. Additional thanks are extended to Dr. T. Yokoi (Aichi Gakuin University), Dr. T. Tsubakimoto (Kanagawa Dental College), Dr. E. Nishida (Aichi Gakuin University), Dr. K. Kosaka (Kanagawa Dental College), and Dr. M. Aino (Aichi Gakuin University) for their technical assistance.

References

Bauss O, Sadat-Khonsari R, Fenske C, Engelke W, Schwestka-Polly R (2004) Temporomandibular joint dysfunction in Marfan syndrome. Oral Surg Oral Med Oral Pathol Oral Radiol Endod 97:592–598

Beertsen W, McCulloch CA, Sodek J (1997) The periodontal ligament: a unique, multifunctional connective tissue. Periodontol 2000:20–40

Berry JE, Zhao M, Jin Q, Foster BL, Viswanathan H, Somerman MJ (2003) Exploring the origins of cementoblasts and their trigger factors. Connect Tissue Res 44 (Suppl 1):97–102

Boileau C, Jondeau G, Babron MC, Coulon M, Alexandre JA, Sakai L, Melki J, Delorme G, Dubourg O, Bonaiti-Pellie C, Bourdarias JP, Junienet C (1993) Autosomal dominant Marfan-like connective-tissue disorder with aortic dilation and skeletal anomalies not linked to the fibrillin genes. Am J Hum Genet 53:46–54

Chien HH, Lin WL, Cho MI (1999) Interleukin-1beta-induced release of matrix proteins into culture media causes inhibition of mineralization of nodules formed by periodontal ligament cells in vitro. Calcif Tissue Int 64:402–413

Cho MI, Matsuda N, Lin WL, Moshier A, Ramakrishnan PR (1992) In vitro formation of mineralized nodules by periodontal ligament cells from the rat. Calcif Tissue Int 50:459–467

Cudre-Mauroux C, Occhiodoro T, Konig S, Salmon P, Bernheim L, Trono D (2003) Lentivector-mediated transfer of Bmi-1 and telomerase in muscle satellite cells yields a Duchenne myoblast cell line with long-term genotypic and phenotypic stability. Hum Gene Ther 14:1525–1533

Dietz HC, Cutting GR, Pyeritz RE, Maslen CL, Sakai LY, Corson GM, Puffenberger EG, Hamosh A, Nanthakumar EJ, Curristin SM, Stetten G, Meyers DA, Francomano CA (1991) Marfan syndrome caused by a recurrent de novo missense mutation in the fibrillin gene. Nature 352:337–339

Dimri GP, Martinez JL, Jacobs JJ, Keblusek P, Itahana K, Van Lohuizen M, Campisi J, Wazer DE, Band V (2002) The Bmi-1 oncogene induces telomerase activity and immortalizes human mammary epithelial cells. Cancer Res 62:4736–4745

Flanders KC, Thompson NL, Cissel DS, Van Obberghen-Schilling E, Baker CC, Kass ME, Ellingsworth LR, Roberts AB, Sporn MB (1989) Transforming growth factor-beta 1: histochemical local-

ization with antibodies to different epitopes. J Cell Biol 108: 653–660
Freeman E (1998) Periodontium. In: Ten Cate AR (ed) Oral histology: development, structure, and function, 5th edn. Mosby, St. Louis, pp 253–286
Fujii S, Maeda H, Wada N, Kano Y, Akamine A (2006) Establishing and characterizing human periodontal ligament fibroblasts immortalized by SV40T-antigen and hTERT gene transfer. Cell Tissue Res 324:117–125
Fujita T, Otsuka-Tanaka Y, Tahara H, Ide T, Abiko Y, Mega J (2005) Establishment of immortalized clonal cells derived from periodontal ligament cells by induction of the hTERT gene. J Oral Sci 47:177–184
Fullmer HM, Sheetz JH, Narkates AJ (1974) Oxytalan connective tissue fibers: a review. J Oral Pathol 3:291–316
Giannopoulou C, Cimasoni G (1996) Functional characteristics of gingival and periodontal ligament fibroblasts. J Dent Res 75: 895–902
Haga K, Ohno S, Yugawa T, Narisawa-Saito M, Fujita M, Sakamoto M, Galloway DA, Kiyono T (2007) Efficient immortalization of primary human cells by p16-specific short hairpin RNA or Bmi-1, combined with introduction of hTERT. Cancer Sci 98: 147–154
Handa K, Saito M, Yamauchi M, Kiyono T, Sato S, Teranaka T, Sampath Narayanan A (2002) Cementum matrix formation in vivo by cultured dental follicle cells. Bone 31:606–611
Hewett DR, Lynch JR, Smith R, Sykes BC (1993) A novel fibrillin mutation in the Marfan syndrome which could disrupt calcium binding of the epidermal growth factor-like module. Hum Mol Genet 2:475–477
Itahana K, Zou Y, Itahana Y, Martinez JL, Beausejour C, Jacobs JJ, Van Lohuizen M, Band V, Campisi J, Dimri GP (2003) Control of the replicative life span of human fibroblasts by p16 and the polycomb protein Bmi-1. Mol Cell Biol 23:389–401
Jacobs JJ, Kieboom K, Marino S, DePinho RA, Lohuizen M van (1999) The oncogene and Polycomb-group gene bmi-1 regulates cell proliferation and senescence through the ink4a locus. Nature 397:164–168
Kamata N, Fujimoto R, Tomonari M, Taki M, Nagayama M, Yasumoto S (2004) Immortalization of human dental papilla, dental pulp, periodontal ligament cells and gingival fibroblasts by telomerase reverse transcriptase. J Oral Pathol Med 33:417–423
Kapila YL, Kapila S, Johnson PW (1996) Fibronectin and fibronectin fragments modulate the expression of proteinases and proteinase inhibitors in human periodontal ligament cells. Matrix Biol 15:251–261
Kawamoto T, Shimizu M (2000) A method for preparing 2- to 50-micron-thick fresh-frozen sections of large samples and undecalcified hard tissues. Histochem Cell Biol 113:331–339
Kettle S, Yuan X, Grundy G, Knott V, Downing AK, Handford PA (1999) Defective calcium binding to fibrillin-1: consequence of an N2144S change for fibrillin-1 structure and function. J Mol Biol 285:1277–1287
Kielty CM, Sherratt MJ, Shuttleworth CA (2002) Elastic fibres. J Cell Sci 115:2817–2828
Kosaki K, Udaka T, Okuyama T (2005) DHPLC in clinical molecular diagnostic services. Mol Genet Metab 86:117–123
Kyo S, Nakamura M, Kiyono T, Maida Y, Kanaya T, Tanaka M, Yatabe N, Inoue M (2003) Successful immortalization of endometrial glandular cells with normal structural and functional characteristics. Am J Pathol 163:2259–2269
Maslen CL, Corson GM, Maddox BK, Glanville RW, Sakai LY (1991) Partial sequence of a candidate gene for the Marfan syndrome. Nature 352:334–337
Mecham RP (1991) Elastin synthesis and fiber assembly. Ann N Y Acad Sci 624:137–146
Miyazono K, Ichijo H, Heldin CH (1993) Transforming growth factor-beta: latent forms, binding proteins and receptors. Growth Factors 8:11–22
Mizuguchi T, Collod-Beroud G, Akiyama T, Abifadel M, Harada N, Morisaki T, Allard D, Varret M, Claustres M, Morisaki H, Ihara M, Kinoshita A, Yoshiura K, Junien C, Kajii T, Jondeau G, Ohta T, Kishino T, Furukawa Y, Nakamura Y, Niikawa N, Boileau C, Matsumoto N (2004) Heterozygous TGFBR2 mutations in Marfan syndrome. Nat Genet 36:855–860
Neptune ER, Frischmeyer PA, Arking DE, Myers L, Bunton TE, Gayraud B, Ramirez F, Sakai LY, Dietz HC (2003) Dysregulation of TGF-beta activation contributes to pathogenesis in Marfan syndrome. Nat Genet 33:407–411
Ng CM, Cheng A, Myers LA, Martinez-Murillo F, Jie C, Bedja D, Gabrielson KL, Hausladen JM, Mecham RP, Judge DP, Dietz HC (2004) TGF-beta-dependent pathogenesis of mitral valve prolapse in a mouse model of Marfan syndrome. J Clin Invest 114: 1586–1592
Nohutcu RM, McCauley LK, Koh AJ, Somerman MJ (1997) Expression of extracellular matrix proteins in human periodontal ligament cells during mineralization in vitro. J Periodontol 68:320–327
Nollen GJ, Mulder BJ (2004) What is new in the Marfan syndrome? Int J Cardiol 97 (Suppl 1):103–108
Pyeritz RE (2000) The Marfan syndrome. Annu Rev Med 51:481–510
Ramirez RD, Morales CP, Herbert BS, Rohde JM, Passons C, Shay JW, Wright WE (2001) Putative telomere-independent mechanisms of replicative aging reflect inadequate growth conditions. Genes Dev 15:398–403
Saito Y, Yoshizawa T, Takizawa F, Ikegame M, Ishibashi O, Okuda K, Hara K, Ishibashi K, Obinata M, Kawashima H (2002) A cell line with characteristics of the periodontal ligament fibroblasts is negatively regulated for mineralization and Runx2/Cbfa1/Osf2 activity, part of which can be overcome by bone morphogenetic protein-2. J Cell Sci 115:4191–4200
Saito M, Handa K, Kiyono T, Hattori S, Yokoi T, Tsubakimoto T, Harada H, Noguchi T, Toyoda M, Sato S, Teranaka T (2005) Immortalization of cementoblast progenitor cells with Bmi-1 and TERT. J Bone Miner Res 20:50–57
Sawada T, Sugawara Y, Asai T, Aida N, Yanagisawa T, Ohta K, Inoue S (2006) Immunohistochemical characterization of elastic system fibers in rat molar periodontal ligament. J Histochem Cytochem 54:1095–1103
Shen ZJ, Kim SK, Jun DY, Park W, Kim YH, Malter JS, Moon BJ (2007) Antisense targeting of TGF-beta1 augments BMP-induced upregulation of osteopontin, type I collagen and Cbfa1 in human Saos-2 cells. Exp Cell Res 313:1415–1425
Sherr CJ, DePinho RA (2000) Cellular senescence: mitotic clock or culture shock? Cell 102:407–410
Shiga M, Kapila YL, Zhang Q, Hayami T, Kapila S (2003) Ascorbic acid induces collagenase-1 in human periodontal ligament cells but not in MC3T3-E1 osteoblast-like cells: potential association between collagenase expression and changes in alkaline phosphatase phenotype. J Bone Miner Res 18:67–77
Staszyk C, Gasse H (2004) Oxytalan fibres in the periodontal ligament of equine molar cheek teeth. Anat Histol Embryol 33:17–22
Straub AM, Grahame R, Scully C, Tonetti MS (2002) Severe periodontitis in Marfan's syndrome: a case report. J Periodontol 73: 823–826
Ten Cate AR (1998) Hard tissue formation and destruction. In: Ten Cate AR (ed) Oral histology: development, structure, and function, 5th edn. Mosby, St. Louis, pp 69–77
Udaka T, Samejima H, Kosaki R, Kurosawa K, Okamoto N, Mizuno S, Makita Y, Numabe H, Toral JF, Takahashi T, Kosaki K (2005) Comprehensive screening of CREB-binding protein gene mutations among patients with Rubinstein-Taybi syndrome using